Cell Death and Differentiation (2012) 19, 267–273

www.nature.com/cdd

# VDAC1 selectively transfers apoptotic $Ca^{2+}$ signals to mitochondria

D De Stefani[1], A Bononi[2], A Romagnoli[1], A Messina[3], V De Pinto[3], P Pinton[2] and R Rizzuto*[,1]

**Voltage-dependent anion channels (VDACs) are expressed in three isoforms, with common channeling properties and different roles in cell survival. We show that VDAC1 silencing potentiates apoptotic challenges, whereas VDAC2 has the opposite effect. Although all three VDAC isoforms are equivalent in allowing mitochondrial $Ca^{2+}$ loading upon agonist stimulation, VDAC1 silencing selectively impairs the transfer of the low-amplitude apoptotic $Ca^{2+}$ signals. Co-immunoprecipitation experiments show that VDAC1, but not VDAC2 and VDAC3, forms complexes with $IP_3$ receptors, an interaction that is further strengthened by apoptotic stimuli. These data highlight a non-redundant molecular route for transferring $Ca^{2+}$ signals to mitochondria in apoptosis.**

*Cell Death and Differentiation* (2012) **19,** 267–273; doi:10.1038/cdd.2011.92; published online 1 July 2011

Voltage-dependent anion channels (VDACs), the most abundant proteins of the outer mitochondrial membrane (OMM), mediate the exchange of ions and metabolites between the cytoplasm and mitochondria, and are key factors in many cellular processes, ranging from metabolism regulation to cell death. VDACs are high-conductance, weakly anion-selective channel, fully open at low potential, but switching to cation selectivity and lower conductance at higher potentials ('closed' state). Multicellular organisms and mammals have three distinct VDAC genes (VDAC1, VDAC2 and VDAC3), with high sequence homology and similar structure. The recently solved 3D-structure of VDAC1[1–3] shows a $\beta$-barrel membrane protein composed of 19 $\beta$-strands with a regulatory $\alpha$-helix N-terminal domain residing inside the pore.

Besides its fundamental role as metabolite exchanger, the pleiotropic role of VDACs appears to rely on their ability to engage protein-protein interactions with different partners. Indeed, VDACs have been shown to interact with cytoskeletal elements such as actin and tubulin,[4,5] metabolic enzymes,[6] Bcl2-family members including Bak,[7] Bad,[8] tBid[9] and Bcl-xL[10] or other channels such as ANT,[11] or the $IP_3R$.[12,13] This scenario is further complicated by evidence showing that VDAC contribution to cell death can be isoform and stimulus dependent: VDAC1 acts predominantly as a pro-apoptotic protein[14–17] whereas VDAC2 protects from a number of apoptosis inducers,[18] but concurrently appears to be necessary for tBid-mediated cell-death.[9] However, these different effects are not supported by the apparent redundancy in the electrophysiological properties of the isoforms.[19,20]

Mitochondrial $[Ca^{2+}]$ is commonly regarded as an important determinant in cell sensitivity to apoptotic stimuli.[21] Indeed, mitochondrial $Ca^{2+}$ accumulation acts as a 'priming signal' sensitizing the organelle and promoting the release of caspase cofactors, both in isolated mitochondria as well as in intact cells.[22,23] In this context, ER-mitochondria contacts mediate the tight and efficient $Ca^{2+}$ transmission between the two organelles and thus could represent a potential regulatory site for cell death signals.[24] Here we investigate the role of the different VDAC isoforms in the context of cell sensitivity to apoptosis and their role in regulating ER-mitochondrial $Ca^{2+}$ signals transmission, and demonstrated that VDAC1, by selectively interacting with the $IP_3Rs$, is preferentially involved in the transmission of the low-amplitude apoptotic $Ca^{2+}$ signals to mitochondria.

## Results

In this work, we aimed to correlate the $Ca^{2+}$ channeling properties of the VDAC isoforms with their effects on cell death. We first downregulated the individual isoforms by RNAi silencing (Figure 1c). The siRNA of interest was co-transfected with a GFP reporter, and the effect on cell fate was evaluated by applying an apoptotic challenge (C2-ceramide or $H_2O_2$) and comparing the survival of transfected and non-transfected cells. In these experiments, the siRNA of interest was co-transfected with a GFP reporter and the percentage of GFP-positive cells was calculated before and after applying an apoptotic stimulus (C2-ceramide

[1]Department of Biomedical Sciences, University of Padova and CNR Neuroscience Institute, Padua, Italy; [2]Department of Experimental and Diagnostic Medicine, Interdisciplinary Center for the Study of Inflammation and BioPharmaNet, University of Ferrara, Ferrara, Italy and [3]Department of Biology, Section of Molecular Biology, University of Catania and National Institute of Biostructures and Biosystems, Catania, Italy
*Corresponding author: R Rizzuto, Department of Biomedical Sciences, University of Padova and CNR Neuroscience Institute, Via G.Colombo 3, Padua 35131, Italy. Tel: +390498276061; Fax: +390498276049; E-mail: rosario.rizzuto@unipd.it
**Keywords:** mitochondria; calcium; apoptosis; VDAC1
**Abbreviations:** $[Ca^{2+}]_{cyt}$, cytosolic $[Ca^{2+}]$; $[Ca^{2+}]_{ER}$, endoplasmic reticulum $[Ca^{2+}]$; $[Ca^{2+}]_{mt}$, mitochondrial $[Ca^{2+}]$; cytAeq, cytosolic aequorin; ER, endoplasmic reticulum; erAeqMut, endoplasmic reticulum-targeted mutated aequorin; GFP, green fluorescent protein; $IP_3R$, inositol 1,4,5-trisphosphate receptor; mtAeqMut, mitochondrially targeted mutated aequorin; mtAeqwt, mitochondrially targeted aequorin; mtGFP, mitochondrially targeted green fluorescent protein; OMM, outer mitochondrial membrane; PGC-1, peroxisome-proliferator activated receptor coactivator-1; siRNA, small interfering RNA; TMRM, tetramethylrhodamine methyl esther; VDAC, voltage-dependent anion channel
Received 22.10.10; revised 22.4.11; accepted 10.5.11; Edited by M Piacentini; published online 01.7.11

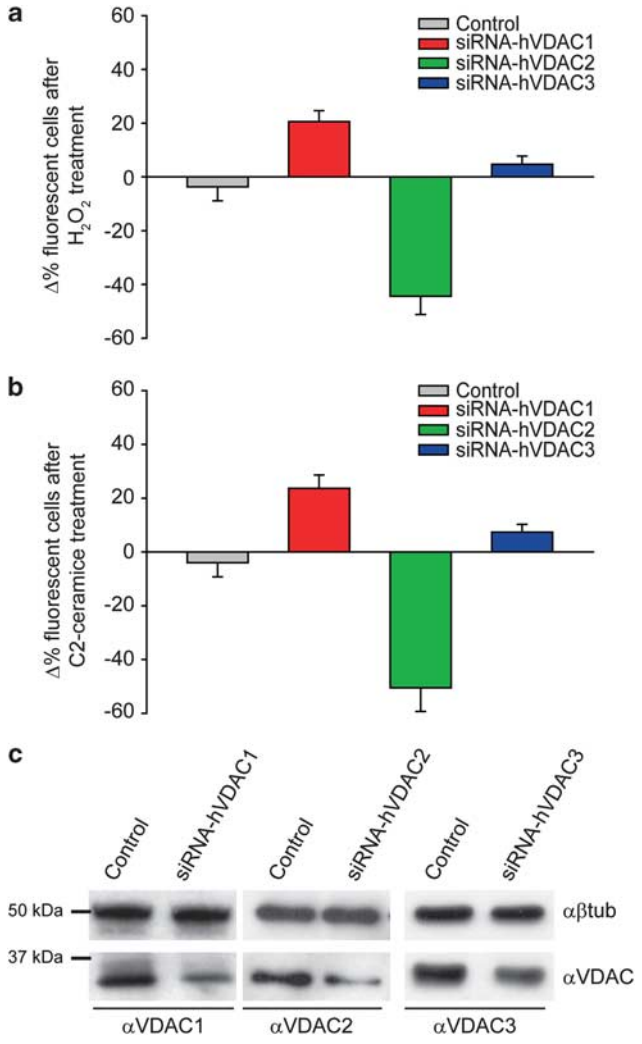


**Figure 1** Sensitivity to apoptotic challenges of VDAC-silenced cells. Cells were co-transfected with a fluorescent marker (GFP) and the siRNA of interest. The graph bar shows the change in percentage of fluorescent cells before the treatment with 100 $\mu$M $H_2O_2$ for 2 h ((**a**) control $-3.7 \pm 5.2\%$; siRNA-hVDAC1 $20 \pm 4.1\%$; siRNA-hVDAC2 $-44.4 \pm 6.8\%$; siRNA-hVDAC3 $+4.7 \pm 3.1\%$) and 30 $\mu$M C2-ceramide for 2 h ((**b**) control $-4 \pm 5.3\%$; siRNA-hVDAC1 $+24.3 \pm 5.1\%$; siRNA-hVDAC2 $-50.1 \pm 6.8\%$; siRNA-hVDAC3 $+7.1 \pm 2.5\%$). (**c**) HeLa cells were transfected for 48 h with control or siRNA-hVDAC encoding plasmid. Cells were harvested, total protein was extracted and subjected to western blotting analysis with antibodies anti-$\beta$-tubulin as loading control and anti-VDAC specific antibodies as indicated

or $H_2O_2$). In mock-transfected cells, although the total number of cells is reduced after cell death induction, the apparent transfection efficiency was maintained (i.e. transfected and non-transfected cells have the same sensitivity to the apoptotic stimulus and thus die to the same extent). However, when GFP-positive cells are co-transfected with a construct influencing their sensitivity to apoptosis, this will be reflected by a change in the fraction of fluorescent cells, that is, in the 'apparent' transfection efficiency. Thus, protection from apoptosis results into an apparent increase of transfection, whereas a decrease reflects a higher sensitivity to apoptosis. The results of the experiment are shown in Figure 1. Mock-transfected cells show no difference in the percentage of fluorescent cells after $H_2O_2$ treatment ($-3.7 \pm 5.2\%$), whereas in the same conditions VDAC1-, VDAC2- and VDAC3-silenced GFP-positive cells were varied by $20 \pm 4.1\%$, $-44.4 \pm 6.8\%$ and $4.7 \pm 3.1\%$, respectively (Figure 1a). Similar results were obtained with C2-ceramide (Figure 1b). This confirms the notion that VDAC1 is pro-apoptotic and, among the various reported effects of VDAC2, the pro-survival role is prevailing in HeLa cells. Finally, VDAC3 shows no significant effect on apoptosis.

Considering that the enhancement of mitochondrial $Ca^{2+}$ uptake generally correlates with increased sensitivity to apoptosis[21] and that VDAC1 has been shown to be a regulator of OMM permeability to $Ca^{2+}$,[15] we wondered whether isoform specificity could rely on different $Ca^{2+}$ channeling properties of the VDACs. The individual VDAC siRNAs were thus co-transfected with a mitochondrial $Ca^{2+}$-probe (mtAeqMut). After aequorin reconstitution with the cofactor coelenterazine, cells were challenged with 100 $\mu$M histamine, and luminescence was measured and converted to $Ca^{2+}$, as described in the Materials and Methods section. VDAC1 silencing significantly reduced the histamine-induced $[Ca^{2+}]_{mt}$ peak (Figures 2a and c, $[Ca^{2+}]_{mt}$ peak values: control, $88.6 \pm 2.7$ $\mu$M; siRNA-hVDAC1, $75.6 \pm 3.2$ $\mu$M; siRNA-hVDAC2, $64.9 \pm 3.5$ $\mu$M; siRNA-hVDAC3, $69 \pm 3.8$ $\mu$M). Interestingly, VDAC2 and VDAC3 silencing had the same effect, if anything greater. To confirm this notion, we carried out overexpression experiments, and, also in this case, VDAC1 showed an enhancement of mitochondrial $Ca^{2+}$ uptake, in agreement with previous data.[15] The effect was comparable, if not smaller, than that observed upon overexpression of VDAC2 and VDAC3 (Figures 2b and c, $[Ca^{2+}]_{mt}$ peak values: hVDAC1-EYFP, $97.7 \pm 3.3$ $\mu$M; hVDAC2-EYFP, $102.7 \pm 4.2$ $\mu$M; hVDAC3-EYFP, $112.8 \pm 5.5$ $\mu$M).

To rule out a confounding effect on cytosolic $Ca^{2+}$ signaling, we measured ER and cytosolic $[Ca^{2+}]$ with the appropriate aequorin chimeras. Silencing or overexpression of the three VDAC isoforms did not alter significantly the state of filling of the ER store (Figure 3a), nor of its release kinetics (data not shown). Accordingly, the cytosolic $[Ca^{2+}]$ transient evoked by histamine stimulation was not significantly affected when any isoform were silenced (Figure 3b) or overexpressed (Figure 3c). Finally, mtGFP imaging and mitochondrial loading with the potential sensitive dye tetramethylrhodamine methyl ester (TMRM) showed that the effect was not due to changes in mitochondrial morphology or significant reduction of mitochondrial membrane potential (data not shown). Altogether, these data, while showing a clear effect of VDAC silencing or overexpression on mitochondrial $Ca^{2+}$ handling, argue against the possibility that the pro-apoptotic effect of VDAC1 depends on a greater $Ca^{2+}$ conductance of this isoform. Rather, the data may suggest a preferential role of the VDAC2 and VDAC3 isoforms in $Ca^{2+}$ transport (also considering their lower expression levels[25]), although the real significance of this observation could be hampered by differences in protein stability or trafficking to the OMM.

The pro-apoptotic activity of VDAC1 thus appears either totally independent of $Ca^{2+}$, or due to the fine tuning of $Ca^{2+}$ signals in specialized microdomains that may be overlooked in bulk cytosolic measurements.[26] We followed the latter

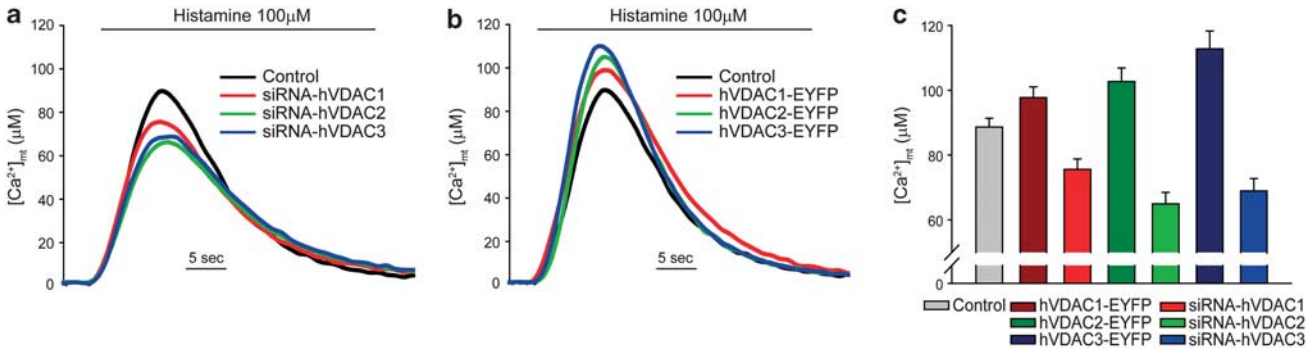


**Figure 2** Effect of VDAC isoform silencing or overexpression on mitochondrial $Ca^{2+}$ uptake. $[Ca^{2+}]_{mt}$ increase evoked by histamine stimulation in VDAC-silenced (**a** and **c**) or VDAC-overexpressing (**b** and **c**) cells ($[Ca^{2+}]_{mt}$ peak values: control, 88.6 ± 2.7 $\mu$M; siRNA-hVDAC1, 75.6 ± 3.2 $\mu$M; siRNA-hVDAC2, 64.9 ± 3.5 $\mu$M; siRNA-hVDAC3, 69 ± 3.8 $\mu$M; hVDAC1-EYFP, 97.7 ± 3.3 $\mu$M; hVDAC2-EYFP, 102.7 ± 4.2 $\mu$M; hVDAC3-EYFP, 112.8 ± 5.5 $\mu$M). (**a** and **b**) Representative traces, (**c**) bar graph of the average $[Ca^{2+}]_{mt}$ peak. The traces are representative of >12 experiments that gave similar results. The bar graphs are the average of all experiments performed

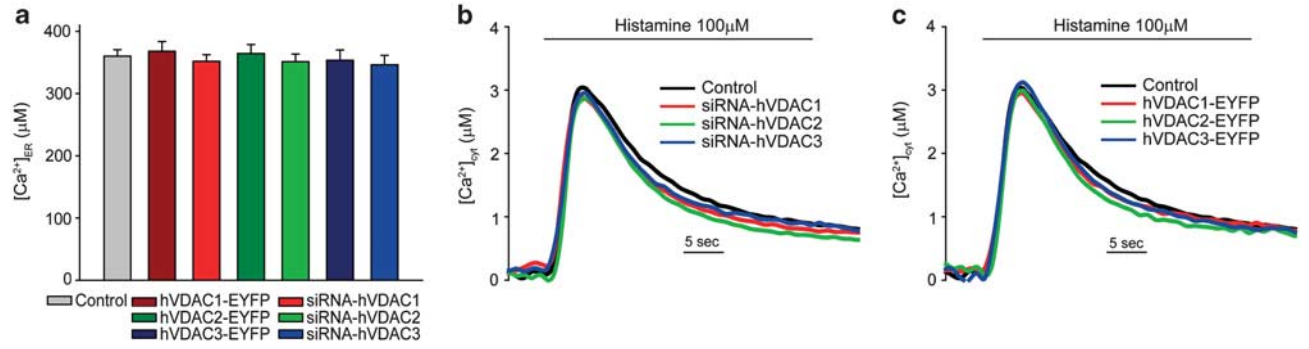


**Figure 3** Effect of VDAC isoform silencing or overexpression on ER and cytosolic $[Ca^{2+}]$. (**a**) Effect of the overexpression, or silencing, of individual VDAC isoforms on $[Ca^{2+}]_{ER}$ steady-state levels (control, 360.1 ± 10.5 $\mu$M; siRNA-hVDAC1, 351.9 ± 10.6 $\mu$M; siRNA-hVDAC2, 352.3 ± 12.3 $\mu$M; siRNA-hVDAC3, 346.5 ± 15.1 $\mu$M; hVDAC1-EYFP, 368 ± 15.6 $\mu$M; hVDAC2-EYFP, 364.5 ± 14.4 $\mu$M and hVDAC3-EYFP, 353.6 ± 16.6 $\mu$M). Transfection with the appropriate aequorin probe, reconstitution and $[Ca^{2+}]$ measurements were carried out as detailed in the methods section. When indicated, the cells were challenged with 100 $\mu$M histamine. erAEQ transfection and $[Ca^{2+}]_{ER}$ measurements, after ER $Ca^{2+}$ depletion, aequorin reconstitution and ER refilling were carried out as detailed in the methods section. (**b** and **c**) Representative traces of cytosolic $Ca^{2+}$ transients evoked by 100 $\mu$M histamine in VDAC-silenced (**b**) and overexpressing (**c**) cells ($[Ca^{2+}]_{cyt}$ peak values: control, 3.06 ± 0.05 $\mu$M; siRNA-hVDAC1, 2.85 ± 0.06 $\mu$M; siRNA-hVDAC2, 2.81 ± 0.07 $\mu$M; siRNA-hVDAC3, 2.98 ± 0.06 $\mu$M; hVDAC1-EYFP, 2.94 ± 0.06 $\mu$M; hVDAC2-EYFP, 2.97 ± 0.07 $\mu$M and hVDAC3-EYFP, 3.08 ± 0.04 $\mu$M). The traces and graph bars of this figure are representatives of >12 experiments that gave similar results

possibility, based on growing evidence demonstrating that the mitochondria/ER crosstalk is not merely the consequence of physical neighborhood but relies on the existence of macromolecular complexes linking the two organelles.[27,28] Specifically, during massive $Ca^{2+}$ release upon maximal agonist stimulation, the existence of discrete signaling units could be overwhelmed and masked by the robustness of the response. Conversely, when an apoptotic stimulus causes a small, sustained $Ca^{2+}$ release the existence of preferential channeling routes could become relevant. Based on previous data, showing the interaction of the $IP_3R$ with VDAC mediated by the grp75 chaperone,[12] we investigated whether $IP_3Rs$ and grp75 preferentially interact with VDAC1, forming privileged signaling units. We first performed co-immunoprecipitation experiments using the highly expressed $IP_3R$ type 3 ($IP_3R$-3) as bait. Strikingly, Figure 4a shows that VDAC1 is the only isoform bound to the $IP_3R$ in stringent conditions: no VDAC2 or VDAC 3 could be detected, also in long-term exposures. Neither actin, nor hexokinase-I, a known interactor of VDAC1, were co-immunoprecipitated in the assay, whereas the grp75 chaperone did. To confirm the specificity of the interaction, we also carried out the reverse experiment, by immunoprecipitating VDAC1 and revealing the presence of grp75 and $IP_3R$-3 in the precipitate. In these experiments, the cells were transfected with an HA-tagged VDAC1 fusion protein, and immunoprecipitation was carried out with anti-HA antibodies. The results, shown in Figure 4b, demonstrate that both $IP_3R$-3 and grp75 co-immunoprecipitate with VDAC1 (similarly to previous data with the $IP_3R$-1,[12] and see also Figure 5c). We then investigated whether the VDAC1-$IP_3Rs$ interaction is altered in apoptotic conditions. We thus performed co-immunoprecipitations in cells challenged with $H_2O_2$ using grp75 or VDAC1-HA as bait. VDAC1 pull-down in $H_2O_2$-treated cells resulted in a significantly greater amount of both grp75 and $IP_3R$ in the immunoprecipitate (Figure 5a), and the relative amount of $IP_3R$ co-immunoprecipitating with grp75 was significantly greater in $H_2O_2$-treated cells (Figure 5b). Moreover, we performed co-immunoprecipitation experiments also with $IP_3R$ type 1: as shown in Figure 5c, similarly to $IP_3R$-3, also $IP_3R$-1 interacts with VDAC1 but not with VDAC2, and $H_2O_2$ treatment enhance this interaction (although the effect seems weaker than with $IP_3R$-3).

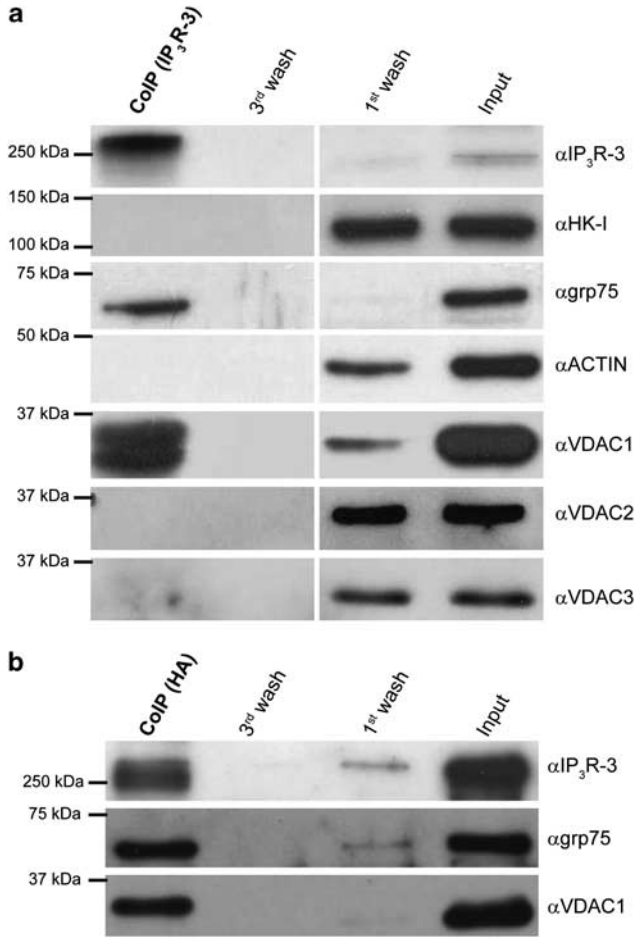


**Figure 4** Co-immunoprecipitations of VDAC1 with $IP_3R$-3. Co-immunoprecipitations using $IP_3R$-3 (**a**) and VDAC1-HA (**b**) as baits. HeLa cells were grown in 10-cm Petri dishes until full confluence. For VDAC1-HA immunoprecipitation, cells were transfected 48 h before experiment. Cells were then detached by scraping, harvested and proteins were extracted in non-denaturing conditions as indicated in the methods section. After protein quantification, 700 $\mu$g were incubated overnight at 4 °C with the 3 $\mu$g of the indicated antibody. The immunocomplex was then isolated by adding protein G-coated sepharose beads for 2 h at 4 °C. The purified immunocomplex was then washed three times with lysis buffer. Indicated fractions were then subjected to SDS-PAGE and western blotting, and probed with the indicated antibodies

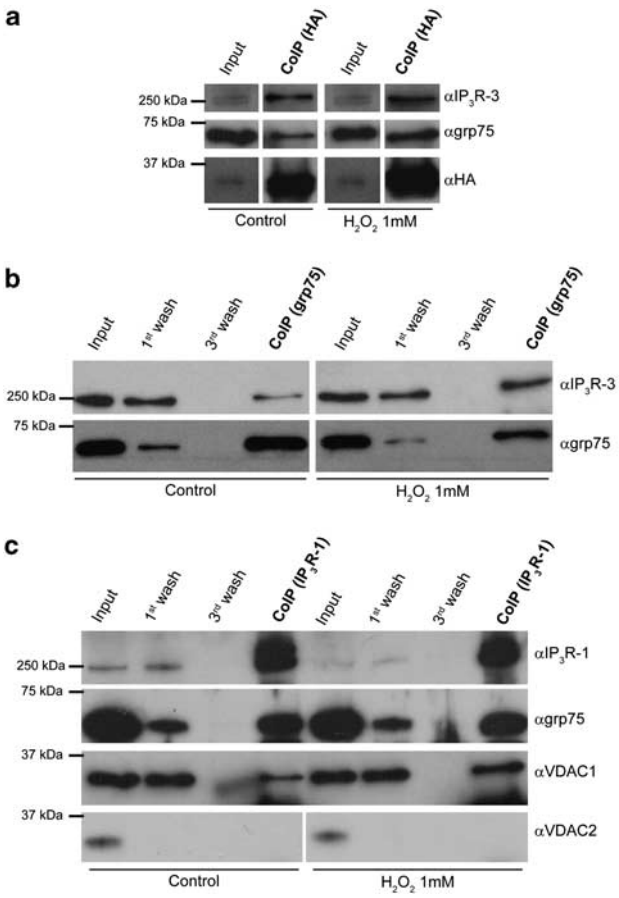


**Figure 5** Co-immunoprecipitations of VDAC1 with $IP_3R$-3 after $H_2O_2$ treatment. Co-immunoprecipitations using VDAC1-HA (**a**), grp75 (**b**) and $IP_3R$-1 (**c**) as baits. HeLa cells were grown in 10-cm Petri dishes until full confluence. For VDAC1-HA immunoprecipitation, cells were transfected 48 h before experiment. Cells were then detached by scraping, harvested, incubated for 10 min with vehicle or 1 mM $H_2O_2$ and proteins were extracted in non-denaturing conditions as indicated in the methods section. After protein quantification, 700 $\mu$g were incubated overnight at 4 °C with the 3 $\mu$g of the indicated antibody. The immunocomplex was then isolated by adding protein G- (for anti-HA) or A- (for anti-$IP_3R$-1 and grp75) coated sepharose beads for 2 h at 4 °C. The purified immunocomplex was then washed three times with lysis buffer. Indicated fractions were then subjected to SDS-PAGE and western blotting, and probed with the indicated antibodies

In order to test whether the interaction of VDAC1 and $IP_3Rs$ is involved in apoptotic signaling, we investigated the $Ca^{2+}$ transients evoked by apoptotic stimuli in VDAC-silenced cells. We applied an oxidative stress, that is, treated the cells acutely with 1 mM $H_2O_2$. As previously reported,[23] the addition of $H_2O_2$ caused a $[Ca^{2+}]_{cyt}$ increase that is much smaller and more sustained than that evoked by histamine (Figures 6a and b). Under those conditions, mitochondria also undergo a small increase (peak value $<1\,\mu$M). VDAC1 silencing decreased mitochondrial $Ca^{2+}$ accumulation, while the knock-down of the other isoforms was indistinguishable from controls. We then titrated the histamine concentration in order to elicit a small $Ca^{2+}$ response, comparable to that evoked by $H_2O_2$ by applying a 0.5 $\mu$M histamine challenge. Under those conditions, no difference among the different VDAC isoforms could be revealed (Figure 6c), thus suggesting that besides the slow kinetics the strengthening of the physical coupling of the $IP_3R$ and VDAC1 channels by apoptotic challenges may have an important role in the potentiation of mitochondrial $Ca^{2+}$ signals and the induction of cell death.

Finally, in order to dissect the precise contribution of the different $IP_3R$ isoforms to the VDAC1-dependent transmission of apoptotic challenges, we investigated the effect of shRNAs against $IP_3R$ type 1 and 3. We first screened a panel of shRNAs, selecting for further studies the two shRNAs (sh$IP_3R$-1#58 and sh$IP_3R$-3#67) that gave $>50\%$ reduction in $IP_3R$-1 and $IP_3R$-3 protein levels, respectively (Figure 7a). We thus tested cellular sensitivity to apoptotic stimuli by carrying out the experiment of Figure 1 in the cells in which $IP_3Rs$ were selectively silenced. Strikingly, while $IP_3R$-1 silencing seems to have no consequence on cell death induced by $H_2O_2$, silencing of the $IP_3R$-3 almost abrogated the protective effect of VDAC1 silencing, thus further demonstrating that $IP_3R$-3 and VDAC1 act on the same signaling route.

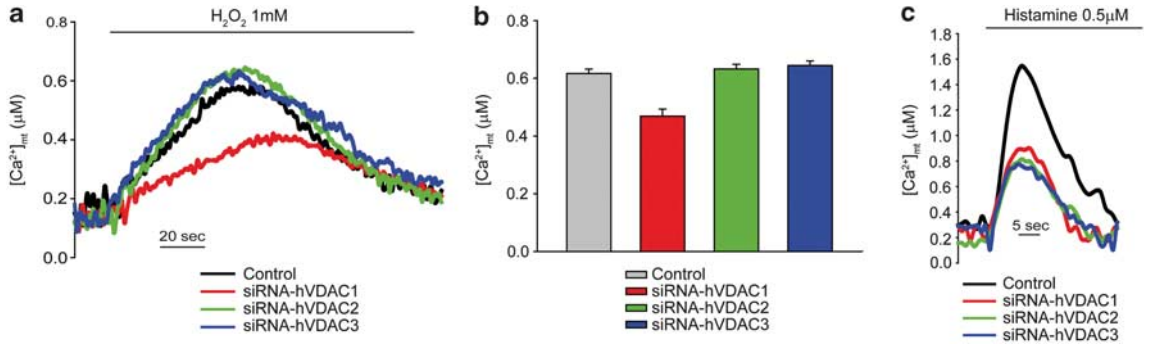


**Figure 6** VDAC1 selectively transfers apoptotic $Ca^{2+}$ signals to mitochondria. Representative traces (**a**) and statistics (**b**) of $[Ca^{2+}]_{mt}$ evoked by the acute administration of 1 mM $H_2O_2$ ($[Ca^{2+}]_{mt}$ peak values: control, 0.617 ± 0.015 $\mu$M; siRNA-hVDAC1, 0.469 ± 0.025 $\mu$M; siRNA-hVDAC2, 0.632 ± 0.016 $\mu$M; siRNA-hVDAC3, 0.644 ± 0.016 $\mu$M). (**c**) $[Ca^{2+}]_{mt}$ increases evoked by 0.5 $\mu$M histamine. All other conditions as in Figure 2

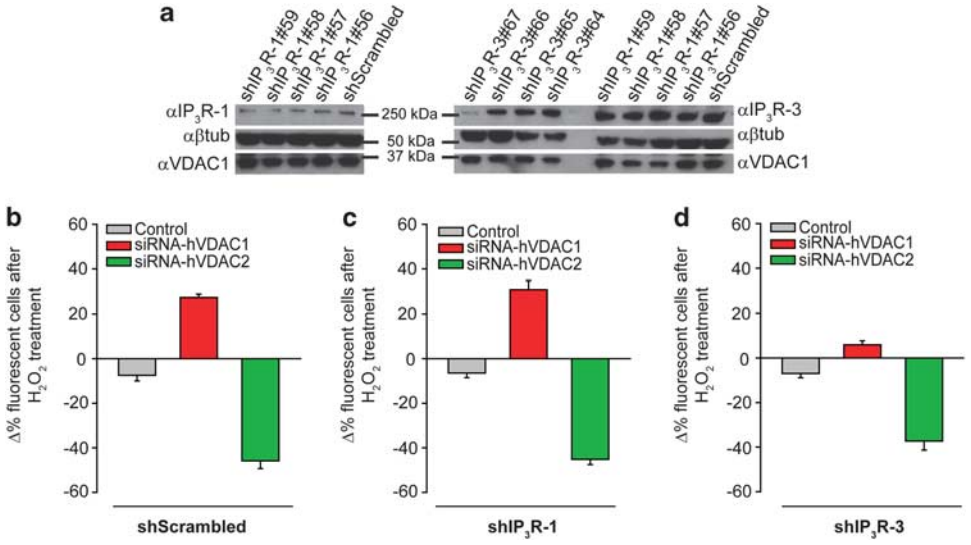


**Figure 7** $IP_3R$-3 silencing abrogates cell death regulation induced by VDAC1. (**a**) HeLa cells were transfected for 72 h with control or different shRNAs against $IP_3R$-1 or $IP_3R$-3. Cells were harvested, total protein was extracted and subjected to western blotting analysis with specific antibodies anti-$IP_3R$-1/3 and anti-$\beta$-Tubulin as loading control. shRNA-$IP_3R$-1#58 and $IP_3R$-3#67 were selected for subsequent experiments. (**b**, **c** and **d**) Cells were co-transfected with one construct containing both the shRNAs for control (**b**, shScrambled), $IP_3R$-1 (**c**, sh$IP_3R$-1), or $IP_3R$-3 (**d**, sh$IP_3R$-3) and a fluorescent marker (GFP), together with the siRNA of interest. The graph bar shows the change in percentage of fluorescent cells before treatment with 100 $\mu$M $H_2O_2$ for 2 h (**b**, Control −7.5 ± 2.5%; siRNA-hVDAC1 27.4 ± 1.5%; siRNA-hVDAC2 −45.9 ± 3.5%; **c**, Control −6.5 ± 2.1%; siRNA-hVDAC1 +30.9 ± 3.9%; siRNA-hVDAC2 −45.2 ± 2.3%; **d**, Control −4 ± 5.3%; siRNA-hVDAC1 +24.3 ± 5.1%; siRNA-hVDAC2 −50.1 ± 6.8%)

## Discussion

Several observations support the notion that VDAC can finely tune cellular processes in an isoform-specific way: (i) selective genetic ablation of the three VDAC genes exhibits different phenotypes;[29] (ii) VDAC1 and VDAC2 exert diametrically opposite effects on apoptosis[15,16,18] and a compound acting through VDAC2, erastin, is effective in tumors harboring Ras mutations;[30] (iii) apoptotic challenges[31] and genomic programs, such as the PGC1-$\alpha$ pathway (De Stefani and Rizzuto, unpublished), differentially regulate the expression of VDAC isoforms; and (iv) the three isoforms are localized to different sub-domains of the OMM.[32] We thus investigated in greater detail the molecular mechanism underlying the different role of VDAC isoforms in apoptosis. The first, obvious explanation of this diversity relied on different $Ca^{2+}$ channeling capacities, given the sensitizing role of $Ca^{2+}$ in the release of caspase activators. Our results ruled out the possibility, by showing relatively minor differences in $Ca^{2+}$ channeling that cannot account for their differential cell death regulation. These minor differences could potentially be due to small variations in $Ca^{2+}$ transport capacities. However, as *in situ* VDAC levels after overexpression or gene silencing are quite difficult to rigorously assess, this conclusion is risky. These data simply support the notion that all VDAC isoforms can similarly transport $Ca^{2+}$ in living cells, and this is not correlated with their effect on apoptosis.

How can we then solve the discrepancy between mitochondrial $Ca^{2+}$ transport and apoptosis regulation? An obvious conclusion is the denial (or, at least the reconsideration) of the classic paradigm linking mitochondrial $Ca^{2+}$ to apoptosis. However, this notion is now supported by broad evidence showing that mitochondrial $Ca^{2+}$ loading favors cell death and signaling molecules reducing or increasing $Ca^{2+}$ signals protect from or enhance apoptosis, respectively.[33] $Ca^{2+}$ in mitochondria, however, is an intrinsically pleiotropic signal,[34] and the final outcome varies widely depending on both the

nature of the stimulus (and hence the '$Ca^{2+}$ signature') and concomitant signaling pathways. Indeed, while physiological stimuli cause the rapid release of $Ca^{2+}$ from internal stores, and thus a large and transient mitochondrial $Ca^{2+}$ uptake, cell death signals have been shown to induce only a modest (even if sustained) $[Ca^{2+}]_{mt}$ increase.[23] This latter event has been proposed to represent a sort of priming signal that conditions and sensitizes mitochondria to otherwise non-lethal stimuli. In this context, the local coupling between ER and mitochondrial $Ca^{2+}$ channels becomes critically relevant: small $Ca^{2+}$ microdomains elicited by apoptotic stimuli such as C2-ceramide strongly relies on the existence of a preferential route transmitting the signal from the ER to the mitochondrion; on the other side, during physiological signals large $Ca^{2+}$ microdomains are generated and this fine channel coupling could be potentially overwhelmed by the vigorous ER $Ca^{2+}$ release. On the ER side, the notion that the accurate discrimination of $Ca^{2+}$ signals mediating diverse effects relies on highly specialized molecular determinants was associated to the observation that the selective knockdown of $IP_3R$-3 impairs cell death signals transmission whereas the silencing of the other two isoforms had almost no effect.[35,36] On the mitochondrial side, we wondered whether a similar selectivity could be associated to the mitochondrial channel repertoire at ER/mitochondria contact sites. The results clearly confirmed this possibility, by demonstrating that VDAC1 is preferentially involved in the transfer of apoptotic stimuli (such as those induced by $H_2O_2$) rather than physiological responses to agonists. Strikingly, our co-immunoprecipitation studies showed that $IP_3R$ selectively interacts with VDAC1, providing a molecular route for the higher sensitivity of the $Ca^{2+}$ transfers. Moreover, this selective interaction appears not static but finely tuned by cellular conditions, as demonstrated by the fact that $H_2O_2$ strengthens the coupling between the ER and mitochondrial $Ca^{2+}$ channels, and by the selective involvement of VDAC1 in the transmission of apoptotic stimuli. Although our biochemical evidences suggest that all $IP_3R$ isoforms are dynamically involved in this process (i.e., both $IP_3R$-1 and $IP_3R$-3 selectively interacts with VDAC1), functional data suggest a preferential role of the $IP_3R$-3 in the transmission of apoptotic stimuli, in agreement with previous reports. Moreover, our data also suggest that the mechanism of the protective effect of VDAC2 on cell death does not involve the transmission of $Ca^{2+}$ signals.

Overall, the data presented in this paper reveal a complex molecular organization underlying VDAC $Ca^{2+}$ channeling properties, and allowing VDAC1 to exert its pro-apoptotic activity. The emerging picture reveals that VDACs represent a fundamental factor in mitochondria physiology, with similar channeling properties shared among its different variants, but also mediating diverse effects through isoform-specific protein-protein interactions and the assembly of highly specialized, higher-order protein complexes. This view accounts for most of experimental data available and finally reconciles apparently contrasting evidence, allowing a deeper insight on mitochondrial regulation of cell life and death.

## Materials and Methods

**Materials.** Antibodies were purchased from the following sources and used at the indicated dilutions: αVDAC1 from Calbiochem (Darmstadt, Germany; 1 : 10 000) and AbNova (Taipei, Taiwan; 1 : 2000); αVDAC2 (1 : 1000), αVDAC3 (1 : 1000) and α$IP_3R$-1 (1 : 1000) from Abcam (Cambridge, UK); αIP3R-3 (1 : 1000) from BD Biosciences (San Jose, CA, USA); αtubulin (1 : 10 000), αactin (1 : 5000) and αHA (1 : 5000) from Sigma-Aldrich (St. Louis, MO, USA); αHK-I (1 : 1000) and αgrp75 (1 : 10 000) from Santa Cruz (Santa Cruz, CA, USA). TMRM was purchased from Invitrogen (Carlsbad, CA, USA). All other chemicals were purchased from Sigma-Aldrich.

**Cell culture and transfection.** In all the experiments HeLa cells were used. Cells were grown in Dulbecco's modified Eagle's medium (Euroclone, Milan, Italy), supplemented with 10% fetal bovine serum (Euroclone) and transfected with a standard calcium–phosphate procedure. For aequorin measurements, the cells were seeded 24 h before transfection onto 13-mm glass coverslips and allowed to grow to 50% confluence before transfection. For cell death experiments, cells were seeded onto 12-well plates 24 h before transfection. For western blot and co-immunoprecipitation experiments cells were grown in 10-cm Petri dishes.

**Plasmid cloning.** For selective VDAC silencing several sequences were cloned and tested for specific silencing efficiency without upregulation of the other isoforms. The most effective sequences were: 5′-AAGCGGGAGCACATTAACCTG-3′ for hVDAC1; 5′-AAGGATGATCTCAACAAGAGC-3′ for hVDAC2; 5′-AAGGGTGGCTTG CTGGCTATC-3′ for hVDAC3. Appropriate oligonucleotides containing the selected sequences were purchased from Sigma-Aldrich and cloned into pSuper (Oligoengine, Seattle, WA, USA) according to manufacturer's instructions. VDAC-YFP isoforms have been cloned in a pEGFP-C3 (Clontech, Palo Alto, CA, USA) mutated to obtain the YFP. hVDAC2 and hVDAC3 have been subcloned EcoRI/SalI into this modified pEYFP-C3 vector from pQE-30 (Qiagen, Hilden, Germany) constructs. hVDAC1 has been directly subcloned BamHI/XhoI into pEYFP-C3. shRNA constructs against $IP_3Rs$ were obtained by using the BLOCK-iT RNAi Express system from Invitrogen. Four different sequences were chosen for both $IP_3R$-1 (miR RNAi Select codes: Hmi409056, Hmi409057, Hmi409058 and Hmi409059) and $IP_3R$-3 (miR RNAi Select codes: Hmi409064, Hmi409065, Hmi409066, and Hmi409067), and cloned into pcDNA6.2-GW/EmGFP-miR vectors following manufacturer's instructions.

**Dynamic *in vivo* $[Ca^{2+}]$ measurements with targeted aequorin probes.** cytAeq-, mtAeqMut-, mtAeqwt- or erAeqMut-expressing cells were reconstituted with coelenterazine for 2 h, transferred to the perfusion chamber where light signal was collected in a purpose-built luminometer and calibrated into $[Ca^{2+}]$ values as previously described.[37] All aequorin measurements were carried out in Krebs–Ringer modified buffer (KRB: 135 mM NaCl, 5 mM KCl, 1 mM $MgSO_4$, 0.4 mM $K_2HPO_4$, 1 mM $CaCl_2$, 5.5 mM glucose, 20 mM HEPES, pH = 7.4) containing 1 mM $CaCl_2$. In the measurement of $H_2O_2$-induced $[Ca^{2+}]$ changes, the high affinity aequorin variant (mtAeqwt) was used and aequorin reconstitution protocol was slightly modified to avoid photon emission due to the direct oxidation of coelenterazine by $H_2O_2$; cells were reconstituted with coelenterazine for 1 h, washed three times with KRB supplemented with 2% bovine serum albumin and then incubated in KRB/$Ca^{2+}$ for an additional hour. For $[Ca^{2+}]_{ER}$ measurements, erAEQmut-transfected cells were reconstituted with coelenterazine n, following ER $Ca^{2+}$ depletion in a solution containing 0 $[Ca^{2+}]$, 500 μM EGTA, 1 μM ionomycin, as previously described. After three washes with KRB supplemented with 2% bovine serum albumin and 1 mM EGTA, cells were perfused with KRB buffer containing 100 μM EGTA. ER refilling was then triggered by perfusing KRB buffer supplemented with 1 mM $CaCl_2$ until equilibrium (steady state) was reached.

**Co-immunoprecipitation.** Co-immunoprecipitations were carried out by using protein A- or protein G-coated sepharose beads (GE Healthcare, Chalfont St. Giles, UK) following manufacturer's instructions. Different protein extraction buffers were used in order to minimize non-specific binding while maximizing antigen extraction. $IP_3R$-3 and $IP_3R$-1 were extracted in a modified RIPA buffer (150 mM NaCl, 1% NP-40, 0.05% SDS, Tris 50 mM, pH = 8) while HA and grp75 were purified in a NP-40 buffer (150 mM NaCl, 1% NP-40, Tris 50 mM, pH = 8), all supplemented with proteases and phosphatases inhibitors (PMSF, complete Protease Inhibitor Cocktail Tablets and PhosSTOP Phosphatase Inhibitor Cocktail Tablets from Roche, Basel, Switzerland). Extracted proteins (700 μg) were first precleared by incubating lysates with sepharose beads for 1 h at 4 °C and the supernatant (referred as Input) was incubated overnight with the antibody at 4 °C. Precipitation of the immune complexes was carried for 2 h at 4 °C and washed three times with the extraction buffer. Fractions were analyzed through standard SDS-PAGE (NuPage 4–12% Bis-Tris Gel, Invitrogen) and western blot techniques.

**Cell death experiment.** Cell sensitivity to apoptotic stimuli was evaluated as previously described.[24] HeLa cells grown on 12-well plates at 30% confluence were co-transfected with GFP and control or siRNA-hVDACs containing plasmids in a 1 : 1 ratio. For the experiments shown in Figure 7, siRNA-hVDACs plasmids were co-transfected with plasmids encoding both an EmGFP and the shRNA of interest (either Scrambled, $IP_3R$-1 or $IP_3R$-3). The effect on cell fate was evaluated by applying an apoptotic challenge (20 $\mu$M C2-ceramide or 100 $\mu$M $H_2O_2$) and comparing the survival of transfected and non-transfected cells. In these experiments, the percentage of GFP-positive cells was calculated before and after applying an apoptotic stimulus (C2-ceramide or $H_2O_2$). In mock-transfected cells, although the total number of cells is reduced after cell death induction, the apparent transfection efficiency was maintained (i.e., transfected and non-transfected cells have the same sensitivity to the apoptotic stimulus and thus die to the same extent). However, when cells are transfected with a construct influencing their sensitivity to apoptosis, this will be reflected by a change in the fraction of fluorescent cells, that is, in the 'apparent' transfection efficiency. Thus, protection from apoptosis results into an apparent increase of transfection, whereas a decrease reflects a higher sensitivity to apoptosis. Data are reported as the mean percentage change in the apparent transfection efficiency after apoptotic challenge compared with vehicle-treated cells. Cells were extensively washed with PBS, stained with DAPI, and two images per field (blue and green fluorescence) were taken at $\times$ 10 magnification (mean transfection efficiency were roughly 30% for all conditions). At least 10 fields per coverslip were randomly imaged and counted. Data presented are the sum of at least two different wells per experimental condition carried out in three different independent experiments.

**Statistical analysis.** Statistical analyses were performed using Student's *t*-test. A *P*-value $\leq 0.05$ was considered significant. All data are reported as means $\pm$ S.E.M.

### Conflict of Interest

The authors declare no conflict of interest.

**Acknowledgements**. This work was supported by grants from the Italian Ministries of Education (PRIN and local funds) and Health, European Union (FP7 'MyoAGE'), Italian Space Agency (ASI), NIH (Grant no. 1P01AG025532-01A1), Cariparo Foundation (Padova), the Italian Association for Cancer Research (AIRC), Telethon-Italy and FISM (Multiple Sclerosis) foundations.

1. Ujwal R, Cascio D, Colletier JP, Faham S, Zhang J, Toro L *et al.* The crystal structure of mouse VDAC1 at 2.3 A resolution reveals mechanistic insights into metabolite gating. *Proc Natl Acad Sci USA* 2008; **105**: 17742–17747.
2. Hiller S, Garces RG, Malia TJ, Orekhov VY, Colombini M, Wagner G. Solution structure of the integral human membrane protein VDAC-1 in detergent micelles. *Science* 2008; **321**: 1206–1210.
3. Bayrhuber M, Meins T, Habeck M, Becker S, Giller K, Villinger S *et al.* Structure of the human voltage-dependent anion channel. *Proc Natl Acad Sci USA* 2008; **105**: 15370–15375.
4. Xu X, Forbes JG, Colombini M. Actin modulates the gating of Neurospora crassa VDAC. *J Membr Biol* 2001; **180**: 73–81.
5. Rostovtseva TK, Bezrukov SM. VDAC regulation: role of cytosolic proteins and mitochondrial lipids. *J Bioenerg Biomembr* 2008; **40**: 163–170.
6. Pastorino JG, Hoek JB. Regulation of hexokinase binding to VDAC. *J Bioenerg Biomembr* 2008; **40**: 171–182.
7. Ren D, Kim H, Tu HC, Westergard TD, Fisher JK, Rubens JA *et al.* The VDAC2-BAK rheostat controls thymocyte survival. *Sci Signal* 2009; **2**: ra48.
8. Roy SS, Madesh M, Davies E, Antonsson B, Danial N, Hajnoczky G. Bad targets the permeability transition pore independent of Bax or Bak to switch between Ca2+-dependent cell survival and death. *Mol Cell* 2009; **33**: 377–388.
9. Roy SS, Ehrlich AM, Craigen WJ, Hajnoczky G. VDAC2 is required for truncated BID-induced mitochondrial apoptosis by recruiting BAK to the mitochondria. *EMBO Rep* 2009; **10**: 1341–1347.
10. Vander Heiden MG, Li XX, Gottleib E, Hill RB, Thompson CB, Colombini M. Bcl-xL promotes the open configuration of the voltage-dependent anion channel and metabolite passage through the outer mitochondrial membrane. *J Biol Chem* 2001; **276**: 19414–19419.
11. Verrier F, Deniaud A, Lebras M, Metivier D, Kroemer G, Mignotte B *et al.* Dynamic evolution of the adenine nucleotide translocase interactome during chemotherapy-induced apoptosis. *Oncogene* 2004; **23**: 8049–8064.
12. Szabadkai G, Bianchi K, Varnai P, De Stefani D, Wieckowski MR, Cavagna D *et al.* Chaperone-mediated coupling of endoplasmic reticulum and mitochondrial Ca2+ channels. *J Cell Biol* 2006; **175**: 901–911.
13. Sano R, Annunziata I, Patterson A, Moshiach S, Gomero E, Opferman J *et al.* GM1-ganglioside accumulation at the mitochondria-associated ER membranes links ER stress to Ca(2+)-dependent mitochondrial apoptosis. *Mol Cell* 2009; **36**: 500–511.
14. Tajeddine N, Galluzzi L, Kepp O, Hangen E, Morselli E, Senovilla L *et al.* Hierarchical involvement of Bak, VDAC1 and Bax in cisplatin-induced cell death. *Oncogene* 2008; **27**: 4221–4232.
15. Rapizzi E, Pinton P, Szabadkai G, Wieckowski MR, Vandecasteele G, Baird G *et al.* Recombinant expression of the voltage-dependent anion channel enhances the transfer of Ca2+ microdomains to mitochondria. *J Cell Biol* 2002; **159**: 613–624.
16. Abu-Hamad S, Sivan S, Shoshan-Barmatz V. The expression level of the voltage-dependent anion channel controls life and death of the cell. *Proc Natl Acad Sci USA* 2006; **103**: 5787–5792.
17. Tomasello F, Messina A, Lartigue L, Schembri L, Medina C, Reina S *et al.* Outer membrane VDAC1 controls permeability transition of the inner mitochondrial membrane in cellulo during stress-induced apoptosis. *Cell Res* 2009; **19**: 1363–1376.
18. Cheng EH, Sheiko TV, Fisher JK, Craigen WJ, Korsmeyer SJ. VDAC2 inhibits BAK activation and mitochondrial apoptosis. *Science* 2003; **301**: 513–517.
19. Xu X, Decker W, Sampson MJ, Craigen WJ, Colombini M. Mouse VDAC isoforms expressed in yeast: channel properties and their roles in mitochondrial outer membrane permeability. *J Membr Biol* 1999; **170**: 89–102.
20. Wu S, Sampson MJ, Decker WK, Craigen WJ. Each mammalian mitochondrial outer membrane porin protein is dispensable: effects on cellular respiration. *Biochim Biophys Acta* 1999; **1452**: 68–78.
21. Rizzuto R, Marchi S, Bonora M, Aguiari P, Bononi A, De Stefani D *et al.* Ca(2+) transfer from the ER to mitochondria: when, how and why. *Biochim Biophys Acta* 2009; **1787**: 1342–1351.
22. Szalai G, Krishnamurthy R, Hajnoczky G. Apoptosis driven by IP(3)-linked mitochondrial calcium signals. *EMBO J* 1999; **18**: 6349–6361.
23. Baumgartner HK, Gerasimenko JV, Thorne C, Ferdek P, Pozzan T, Tepikin AV *et al.* Calcium elevation in mitochondria is the main Ca2+ requirement for mitochondrial permeability transition pore (mPTP) opening. *J Biol Chem* 2009; **284**: 20796–20803.
24. Pinton P, Ferrari D, Rapizzi E, Di Virgilio F, Pozzan T, Rizzuto R. The Ca2+ concentration of the endoplasmic reticulum is a key determinant of ceramide-induced apoptosis: significance for the molecular mechanism of Bcl-2 action. *EMBO J* 2001; **20**: 2690–2701.
25. Yamamoto T, Yamada A, Watanabe M, Yoshimura Y, Yamazaki N, Yamauchi T *et al.* VDAC1, having a shorter N-terminus than VDAC2 but showing the same migration in an SDS-polyacrylamide gel, is the predominant form expressed in mitochondria of various tissues. *J Proteome Res* 2006; **5**: 3336–3344.
26. Giacomello M, Drago I, Bortolozzi M, Scorzeto M, Gianelle A, Pizzo P *et al.* Ca2+ hot spots on the mitochondrial surface are generated by Ca2+ mobilization from stores, but not by activation of store-operated Ca2+ channels. *Mol Cell* 2010; **38**: 280–290.
27. de Brito OM, Scorrano L. Mitofusin 2 tethers endoplasmic reticulum to mitochondria. *Nature* 2008; **456**: 605–610.
28. Csordas G, Renken C, Varnai P, Walter L, Weaver D, Buttle KF *et al.* Structural and functional features and significance of the physical linkage between ER and mitochondria. *J Cell Biol* 2006; **174**: 915–921.
29. Graham BH, Craigen WJ. Genetic approaches to analyzing mitochondrial outer membrane permeability. *Curr Top Dev Biol* 2004; **59**: 87–118.
30. Yagoda N, von Rechenberg M, Zaganjor E, Bauer AJ, Yang WS, Fridman DJ *et al.* RAS-RAF-MEK-dependent oxidative cell death involving voltage-dependent anion channels. *Nature* 2007; **447**: 864–868.
31. Voehringer DW, Hirschberg DL, Xiao J, Lu Q, Roederer M, Lock CB *et al.* Gene microarray identification of redox and mitochondrial elements that control resistance or sensitivity to apoptosis. *Proc Natl Acad Sci USA* 2000; **97**: 2680–2685.
32. Neumann D, Buckers J, Kastrup L, Hell SW, Jakobs S. Two-color STED microscopy reveals different degrees of co-localization between hexokinase-I and the three human VDAC isoforms. *PMC Biophys* 2010; **3**: 4.
33. Pinton P, Giorgi C, Siviero R, Zecchini E, Rizzuto R. Calcium and apoptosis: ER-mitochondria Ca2+ transfer in the control of apoptosis. *Oncogene* 2008; **27**: 6407–6418.
34. Murgia M, Giorgi C, Pinton P, Rizzuto R. Controlling metabolism and cell death: at the heart of mitochondrial calcium signalling. *J Mol Cell Cardiol* 2009; **46**: 781–788.
35. Khan AA, Soloski MJ, Sharp AH, Schilling G, Sabatini DM, Li SH *et al.* Lymphocyte apoptosis: mediation by increased type 3 inositol 1,4,5-trisphosphate receptor. *Science* 1996; **273**: 503–507.
36. Mendes CC, Gomes DA, Thompson M, Souto NC, Goes TS, Goes AM *et al.* The type III inositol 1,4,5-trisphosphate receptor preferentially transmits apoptotic Ca2+ signals into mitochondria. *J Biol Chem* 2005; **280**: 40892–40900.
37. Pinton P, Rimessi A, Romagnoli A, Prandini A, Rizzuto R. Biosensors for the detection of calcium and pH. *Methods Cell Biol* 2007; **80**: 297–325.